

Characterization of Nano-Structured Nickel-Cobalt Ferrites Synthesized By Citrate-Gel Auto Combustion Method

Abdul Gaffoor and D. Ravinder*

Department of Physics Osmania University Hyderabad-500007

Abstract

Nano-ferrites of the composition $Ni_{1-x}Co_xFe_2O_4$ (where $x=0.0, 0.2, 0.4, 0.6, 0.80$ and 1.0) were synthesized at a very low temperature ($180^\circ C$) by Citrate-gel auto combustion method. The synthesized powders were sintered at $500^\circ C$ for four hours in an air and were characterized by X-ray diffraction (XRD) which confirmed the formation of cubic spinel structure of ferrites. The crystallite size was in the range of 20nm to 31nm . Such low nano sized ferrites are desirable for variety of applications like, in magnetic data storage and in etc. Morphological studies by Scanning Electron Microscopy (SEM) revealed formation of largely agglomerated, well defined nano particles of the sample. Elemental composition characterizations of the prepared samples were performed by Energy Dispersive Spectroscopy (EDS) which shows the presence of Ni, Co, Fe and O without precipitating cations.

Keywords: Ni-Co Nano ferrites; Citrate-gel auto combustion; X-ray Diffraction; SEM; EDS;

I. Introduction

Nanoparticles of magnetic ferrites have attracted great research interest because of their applications in permanent magnets, drug delivery, microwave devices and high-density information storage [1–4]. Cobalt ferrite has been extensively investigated because of its interesting magnetic behavior, chemical stability and mechanical hardness [5,6]. Cobalt ferrite, $CoFe_2O_4$, crystallizes in a partially inverse spinel structure [7]. Nickel-ferrite is an inverse spinel magnetic material [8]. Cobalt ferrite is well known hard magnetic material with high coercivity and saturation magnetization while nickel ferrite is soft material with low coercivity and saturation magnetization. Many of these hard and soft magnetic properties make them very promising for candidates for a variety of applications. Nano size ferrites have been prepared by various techniques such as sol-gel combustion, modified oxidation process, forced hydrolysis, hydrothermal process, ball milling and the micro-emulsion method [9–14].

In the present study we prepared Nano-ferrites of the composition $Ni_{1-x}Co_xFe_2O_4$ (where $x=0.0, 0.2, 0.4, 0.6, 0.80$ and 1.0) were synthesized at a very low temperature ($180^\circ C$) by Citrate-gel auto combustion method

II. Experimental Details

The Nano-ferrites of the composition $Ni_{1-x}Co_xFe_2O_4$ (where $x=0.0, 0.2, 0.4, 0.6, 0.80$ and 1.0) were synthesized at a very low temperature ($180^\circ C$) by Citrate-gel auto combustion method by the below mentioned raw materials.

2.1 Raw Materials:

- Nickel Nitrate-99% Pure (AR Grade) ($Ni(NO_3)_2$)
- Cobalt Nitrate-99% Pure (AR Grade) ($Co(NO_3)_2$)
- Ferric Nitrate-99% pure (AR grade) ($Fe(NO_3)_3 \cdot 9H_2O$)
- Citric acid - 99% pure (AR grade) ($C_6H_8O_7 \cdot H_2O$) .
- Ammonia - 99% pure (AR grade) (NH_3)

2.2 The flow chart for the synthesis of lithium nano ferrite:

In this method Nitrates and Citric acid (all are SDFCL-sd fine Chem.Limited 99% pure AR grade) having molar ratio 1:3 were dissolved in deionized water. Citric acid acts as chelating agent and helps in the homogenous distribution of metal ions. The burnt powder was grind in Agate Mortar and Pestle to get a fine Ferrite powder. Finally the burnt powder was calcinated in air at $500^\circ C$ temperature for four hours and cooled to room temperature.

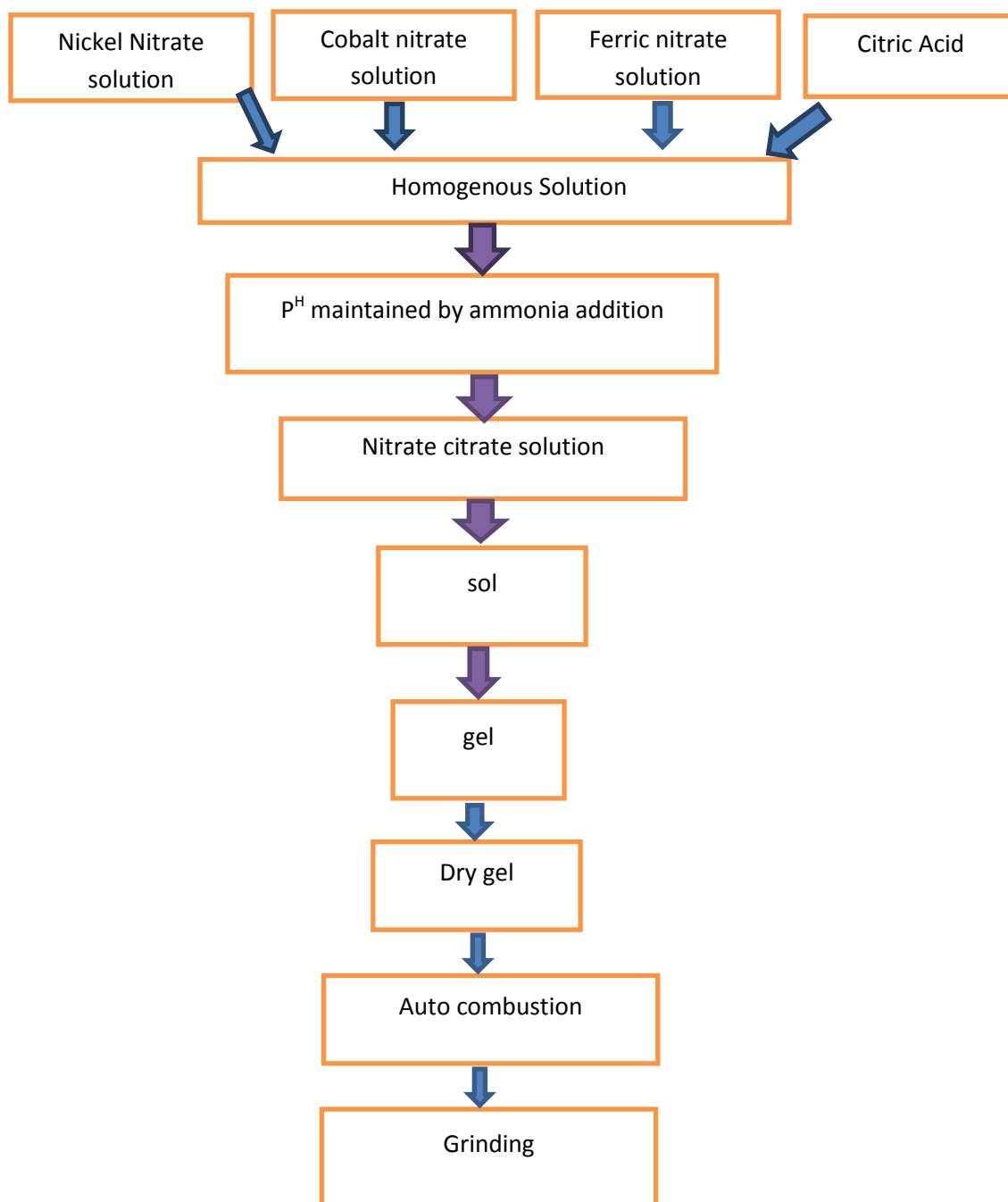


Figure 1 Flow chart for Synthesis of Ni-Co Nano ferrites

2.3. Characterization

X-ray Diffraction with $\text{CuK}\alpha$ ($\lambda = 1.54 \text{ \AA}$) was used to study the single phase nature and nano-phase formation of the Ni-Co ferrite system at room temperature by continuous scanning in the range of 10°C to 90°C .

Micro structural analysis of the prepared samples was carried out by scanning Electron microscopy (SEM) and elemental compositional analysis for all samples was done by Energy Dispersive Spectroscopy (EDS).

III. Results and Discussions

3.1. XRD Analysis

The X-ray diffraction patterns of all the samples were shown in **Figure 2**. XRD patterns and the crystalline phases were identified by comparison with reference data from the JCPDS card No. 742081 for Nickel ferrites (NiFe_2O_4) and JCPDS card No 791744 for Cobalt ferrites (CoFe_2O_4). The XRD patterns of all the Cobalt substituted nickel ferrites showed a homogeneous single phased cubic spinel belonging to the space group $\text{Fd}\bar{3}\text{m}$ (confirmed by

JCPDS card No. 742081). All the Bragg reflections have been indexed, which confirmed the formation of a well defined single phase cubic spinel structure without any impurity peaks. All the peaks are allowed peaks. The strongest reflection has come from (311) plane that indicates spinel phase.

The diffraction peaks can be indexed to the planes of (2 2 0), (3 1 1), (2 2 2), (4 0 0), (5 1 1) and (4 4 0). The observed broadening of diffraction peaks indicates the nano crystallinity of the samples. The particle size of the synthesized ferrite samples was estimated from X-ray peak broadening of diffraction peaks using Scherrer formula [15]. The values of the

particle size, lattice constant and X-ray density as deduced from the X-ray data are given in Table 1

$$t = \frac{0.91\lambda}{\beta \cos \theta}$$

where λ = Wavelength of X-ray, β = Full width and Half Maxima in radians, θ = Bragg's angle at the peak position.

Lattice parameter "a" of individual composition was calculated by using the following formula and values were tabulated in Table 1.

$d = \frac{a}{\sqrt{h^2+k^2+l^2}}$ where a = lattice parameter, d = inter planar distance, hkl = miller indices.

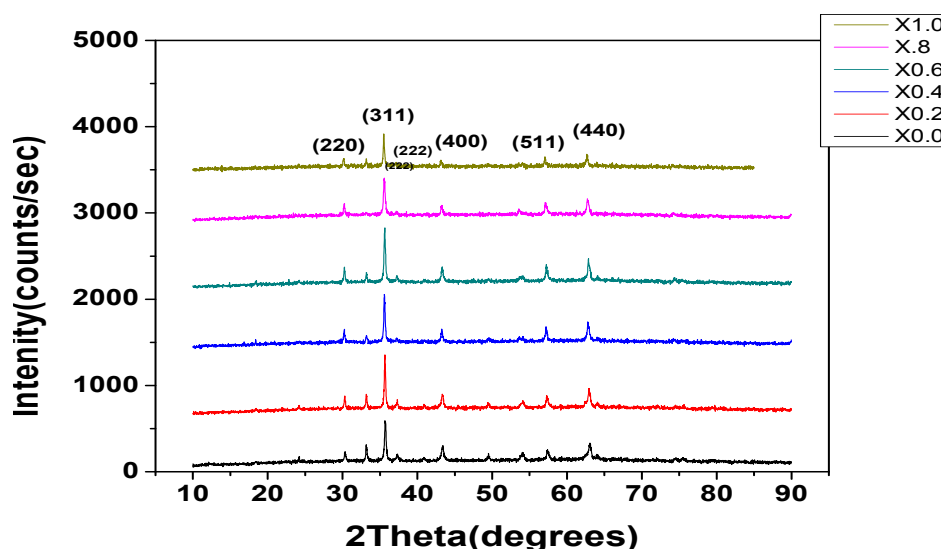


Figure 2. XRD of $Ni_{1-x}Co_xFe_2O_4$ (where $x = 0.0, 0.2, 0.4, 0.6, 0.8, 0$ and 1.0)

The variation of lattice parameter with Co compositions was shown in Figure 3. The lattice parameter was found to increase linearly with increasing Co concentration. This linear variation indicates that the Ni-Co ferrite system obeys Vegard's law [16]. The lattice constant increases with

Cobalt doping, which can be explained based on the relative ionic radius. The ionic radius (oct: 0.82 \AA) of Co^{2+} ions is larger than the ionic radius (oct: 0.78 \AA) of Ni^{2+} ions. Replacement of smaller Ni^{2+} cations with larger Co^{2+} cations causes an increase in lattice constant.

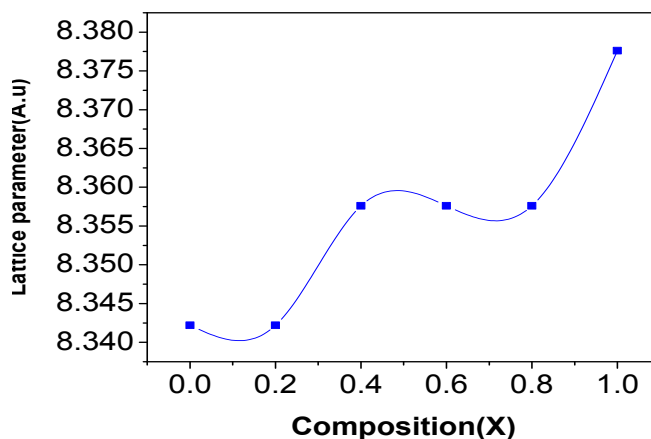


Figure 3 Variation of Lattice Parameter(a) with Composition(x) for Ni-Co nano-ferrites

X-ray density (d_x) for different compositions was calculated using the formula [17] and calculated values were tabulated in Table 2.

$$d_x = \frac{ZM}{Na^3} \text{ gm/cc}$$

where Z = Number of molecules per unit cell (8), M = Molecular weight of the sample, N = Avogadro's Number, a = lattice parameter.

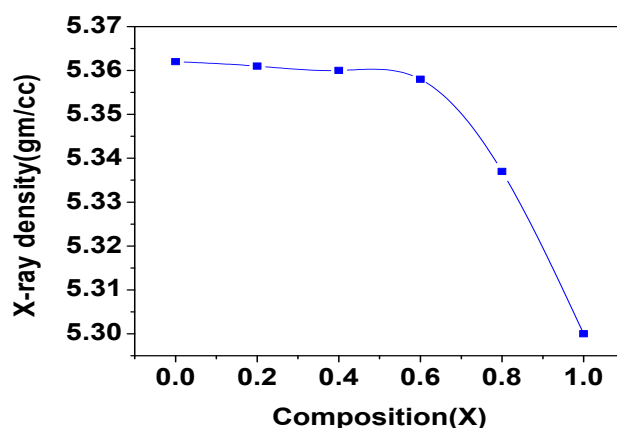


Figure 4 Variation of X-ray density with Composition(X) for Ni-Co-nano-ferrites

The X-ray density is expected to decrease with the Co content because the lattice parameters increase with Co content. Similar result has been observed by Pandit et al. in Mg-Mn ferrites [18] and by M.A. Gabal, et al., in Ni-Mg Nanoferrites by egg white Precursor Method [19]. The decrease in X-ray density can be ascribed to the atomic weight and density of Co^{2+} , which are lower than those of

Ni^{2+} and Fe^{3+} [20].

Volume of unit cell was calculated by using the formula

$V = a^3$ in \AA^3 units where 'a' is lattice parameter. Volume of unit cell was found to increase with increase in Co content, as it depends on lattice parameter which has increased with increase in Co content.

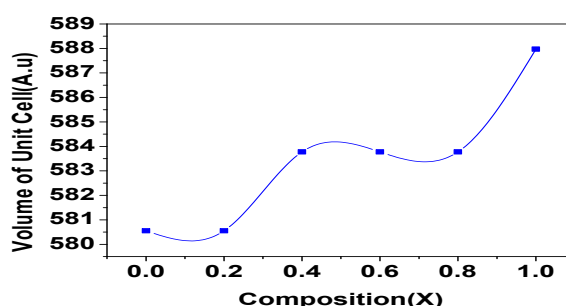


Figure 5 Variation of Volume of Unit cell with Composition(X)

The distance between magnetic ions (hopping length) in A site (tetrahedral) and B site (octahedral) were calculated using the relations $d_A = 0.25a\sqrt{3}$ and $d_B = 0.25a\sqrt{2}$

The calculated values of the hopping length for Tetrahedral site (d_A) and octahedral (d_B) of

different compositions were tabulated in **Table 1**. The relation between hopping length for Octahedral and Tetrahedral sites as a function of Mg content (x) was shown in **Figure 6**. It is observed that the hopping length increases as the Mg content increases.

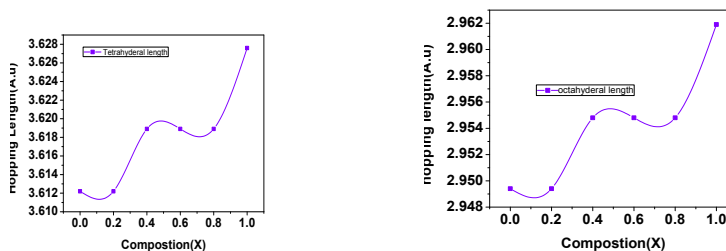


Figure 6 The distance between magnetic ions in both Octahedral and tetrahedral Sites as a function of Composition (X)

Table 1. Values of Crystallite size, Lattice parameter(a),unit cell volume, X-ray density and hopping length for A-Site(d_A) and B-Site(d_B) of Ni-Co Nano ferrite with Composition($X=0.0,0.2,0.4,0.6,0.8,1.0$)

Sample	Particle size(nm)	Lattice parameter(A.u)	Unit cell volume(A.u)	X-Ray density(gm/cc)	A site d_A (A.u)	B Site d_B (A.u)
$NiFe_2O_4$	23.57 nm	8.3422	580.552	5.362	3.6122	2.9494
$Ni_{0.8}Co_{0.2}Fe_2O_4$	30.2 nm	8.3422	580.552	5.360	3.6122	2.9494
$Ni_{0.6}Co_{0.4}Fe_2O_4$	26.37 nm	8.3576	583.773	5.359	3.6189	2.9548
$Ni_{0.4}Co_{0.6}Fe_2O_4$	26.59 nm	8.3576	581.773	5.358	3.6139	2.9507
$Ni_{0.2}Co_{0.8}Fe_2O_4$	20.19 nm	8.3576	583.773	5.337	3.6189	2.9548
$CoFe_2O_4$	25.02 nm	8.3776	587.975	5.300	3.6276	2.9619

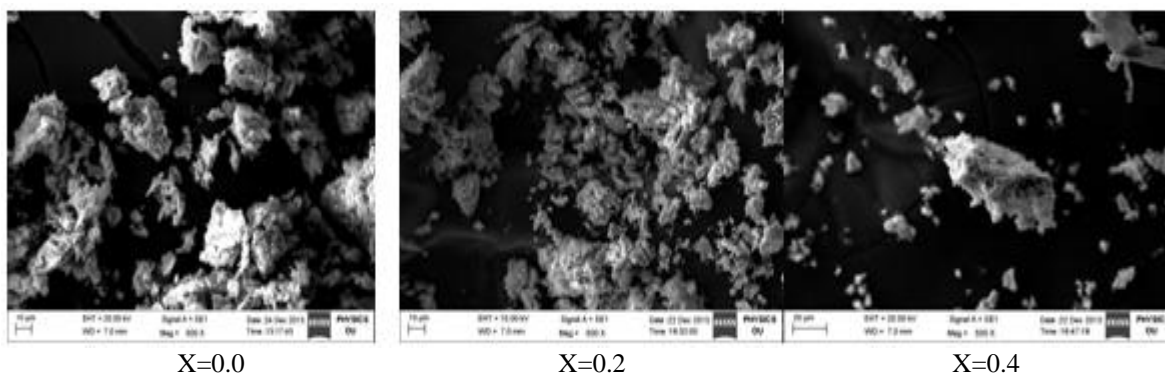
2. Morphology by SEM

Morphology of the prepared samples by Citrate-gel method was studied using scanning electron microscope (SEM) where the secondary electron images were taken at different magnifications to study the morphology. The scanning electron microscopic images of all the synthesized samples were shown in **Figure 7**.

The images show that the particles have an almost homogeneous distribution, and some of them are in agglomerated form. It is evidenced by SEM images that the aggregation of particles lies in nanometric region. The particles were observed as uniform grains (in different SEM images) confirming the crystalline structure of Ni-Co Nanoferrites which were detected by XRD studies. The formation of

Fe_2O_4 was chemically favoured by heating during the synthesis where as final reaction was completed during the sintering where the pores between the particles were removed combined with growth and strong bonds by agglomeration.

It can be seen from SEM micrographs of various compositions that the morphology of the particles is similar. They reveal largely agglomerated, well defined nano particles of the sample powder with inhomogeneous broader grain size distribution. Such broader size distribution is characteristic of mechanically activated nano sized particles. The agglomeration of particles is also because they experience a permanent magnetic moment proportional to their volume [21].



X=0.0

X=0.2

X=0.4

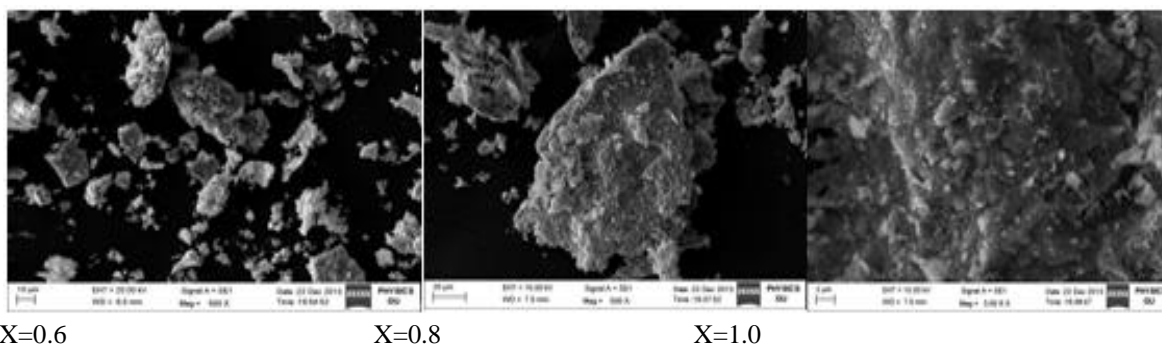


Figure 7 SEM images of Ni_{1-x}Co_xFe₂O₄ Nano ferrites

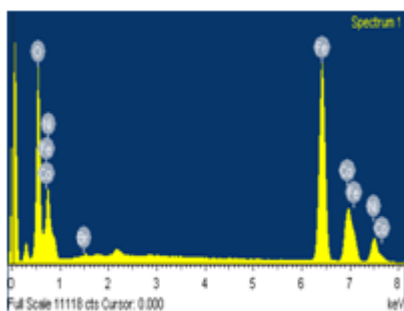
3.3. Elemental Analysis by EDS

The elemental analysis of all the Ni-Co nano ferrite samples with different compositions was analysed by Energy Dispersive Spectrometer (EDS) and the elemental % and atomic % of different elements in the were shown in the **Table 2**. The EDS

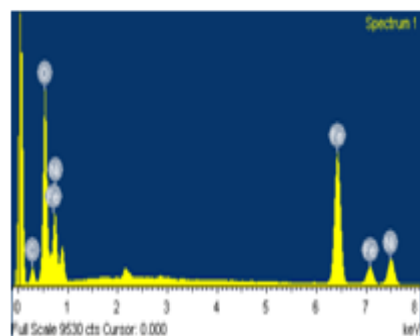
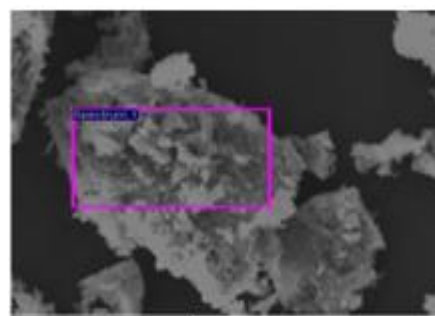
pattern for samples with x = 0.0, 0.4 and 0.8 were shown in **Figure 8** which indicates the elemental and atomic composition in the sample. The compounds show the presence of Ni, Co, Fe and O without precipitating cations.

Table 2 Elements of each sample composition Ni-Co Nano ferrites analysed by (% weight) obtained by EDS

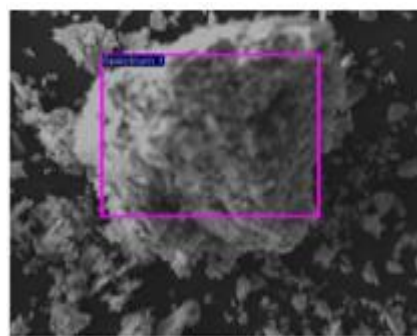
Element Ferrite composition	O		Ni		Co		Fe	
	element % Atomic%		element %	Atomic %	element%	Atomic %	Element %	Atomic %
NiFe ₂ O ₄	29.93	61.88	18.12	9.50	-----	-----	51.92	28.62
Ni _{0.8} Co _{0.2} Fe ₂ O ₄	21.85	49.77	19.31	12.00	6.00	3.71	52.83	34.52
Ni _{0.6} Co _{0.4} Fe ₂ O ₄	28.97	59.23	9.11	5.07	14.91	8.28	46.35	27.15
Ni _{0.4} Co _{0.6} Fe ₂ O ₄	33.38	42.77	12.15	5.70	9.18	4.29	45.28	41.24
Ni _{0.2} Co _{0.8} Fe ₂ O ₄	33.53	51.63	2.69	0.91	11.26	3.80	52.50	43.66
CoFe ₂ O ₄	34.56	66.10	-----	-----	10.88	9.50	46.62	24.34

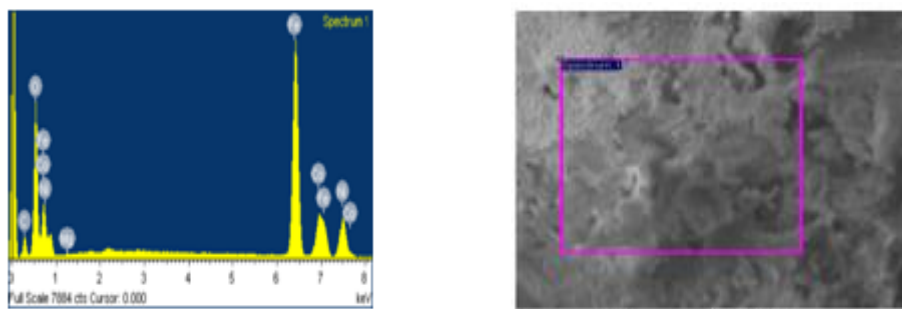


(X=0.0) NiFe₂O₄ Nano ferrite



(X=0.4) Ni_{0.6}Co_{0.4}Fe₂O₄ Nano ferrite





(X=0.8) Ni_{0.2}Co_{0.8}Fe₂O₄ Nano ferrite

Figure 8 EDS graph of Ni_{1-x}Co_xFe₂O₄ Nano ferrites with composition (X=0.0,0.6,1.0)

IV. Conclusions

- Citrate Gel auto combustion technique is a convenient way for obtaining a homogeneous nano sized mixed Ni-Co ferrites.
- The process involves no impurity pickup and material loss. It is a very simple and economical method where no specific heating or cooling rate is required. It is a low temperature processing technique and requires shorter sintering duration.
- X-ray diffraction pattern confirms the formation of cubic spinel structure in single phase without any impurity peak. It is in good agreement with the standard data from ICSD
- The crystallite size of the various Ni-Co ferrites was in the range of 20-31nm.
- The lattice parameter is increased with the increase of Co substitution in Ni-Co ferrites which indicates that the mixed Ni-Co ferrite system obeys Vegard's law.
- SEM micrographs of various compositions indicate the morphology of the particles is similar. They reveal largely agglomerated, well defined nano particles of the sample powder with inhomogeneous broader grain size distribution.
- EDS data gives the elemental% and atomic % in the mixed Ni-Co ferrites and it shows the presence of Ni, Co, Fe and O without precipitating cations

V. Acknowledgments

The authors are very thankful to Prof.K.Venugopal Reddy, Head, Department of Physics, University College of Science, Osmania University, Hyderabad for his support and encouragement to carry out this research work.

Reference

- [1] A.T. Ngo, M.P. Pileni, J. Phys. Chem. B 105 (2001) 53.
- [2] S. Singhal, J. Singh, S.K. Barthwal, K. Chandra, J. Solid State Chem. 178 (2005) 3183.
- [3] M.H. Sousa, F.A. Tourinho, J. Phys. Chem. B 105 (2000) 168.
- [4] K. Raj, R. Moskowitz, R. Casciari, J. Magn. Mater. 149 (1995) 174.
- [5] G. Bate, in: D.J. Craik (Ed.), L Magnetic

- Oxides, Part 2, Wiley Inter Science, New York, 1975, p. 703.
- [6] M.P. Sharrock, IEEE Trans. Magn. 25 (1989) 374.
- [7] K. Haneda, A.H. Morrish, J. Appl. Phys. 63 (1988) 4258.
- [8] D.S.Mathew, R.S.Juang, Chem. Eng.J.129 (2007) 51-65.
- [9] P. Tailhades, C. Villette, A. Rousset, G.U. Kulkarni, K.P. Kannan, C.N.R. Rao, M. Lenglet, J. Solid State Chem. 141 (1998) 56.
- [10] Y. Ahn, E.J. Choi, S. Kim, H.N. Ok, Mater. Lett. 50 (2001) 47.
- [11] N. Hanh, O.K. Quy, N.P. Thuy, L.D. Tung, L. Spinu, Physica B 327 (2003) 382.
- [12] C.N. Chinnasamy, M. Senoue, B. Jeyadevan, O. Perales-Perez, K. Shinoda, K. Tohji, J. Colloid Interf. Sci. 263 (2003) 80.
- [13] M.F.F. Lelis, A.O. Porto, C.M. Goncalves, J.D. Fabris, J. Magn. Mater. 278 (2004) 263.
- [14] K.P. Chae, J. Lee, H.S. Kweon, Y.B. Lee, J. Magn. Mater. 283 (2004) 103.
- [15] B. D. Cullity, "Elements of XR-Diffraction," Addison Wesley Publishing, Reading, 1959, p. 132.
- [16] L. Vegard, "The Constitution of Mixed Crystals and the Space Occupied by Atoms," Zeitsch rift für Physics, Vol. 5, No. 17, 1921, pp.17-23.
- [17] R. C. kumbale, P. A. sheikh, S. S. Kamble and Y. D. kolekar, "Effect of Cobalt Substitution on Structural Magnetic and Electric Properties of Nickel Ferrite," Journal of Alloys and Compounds, Vol. 478, No. 1-2, 2009, pp.599-603. doi:10.1016/j.jmmm.2005.03.007
- [18] A.APandit, A.R.Shitre, D.R.shengule, K.M. Jadhav, J. of Mater. Sci.40 [2] (2005) 423-428
- [19] M.A. Gabal, et al., Journal of Magnetism and Magnetic Materials (2014), <http://dx.doi.org/10.1016/j.jmmm.2014.03.007i>
- [20] C.Kittel, introduction to solid state physics, seventh Ed., Wiley, Singapore (1996).
- [21] Suryawanshi. S. S; Deshpand. V; Sawantn. S.R, J.Mater. Chem. Phy. 1999, 59, 199Doi: [10.1016/S0254-0584\(99\)00046-2](https://doi.org/10.1016/S0254-0584(99)00046-2)